

Contents lists available at [SciVerse ScienceDirect](http://SciVerse.Sciencedirect.com)

# Biochimica et Biophysica Acta

journal homepage: [www.elsevier.com/locate/bbabio](http://www.elsevier.com/locate/bbabio)

## Small-angle neutron scattering study of the ultrastructure of chloroplast thylakoid membranes – Periodicity and structural flexibility of the stroma lamellae <sup>☆</sup>

Dorthe Posselt <sup>a,\*</sup>, Gergely Nagy <sup>b</sup>, Jacob J.K. Kirkensgaard <sup>a</sup>, Jens K. Holm <sup>a</sup>, Thomas H. Aagaard <sup>a</sup>, Peter Timmins <sup>b</sup>, Eszter Rétfalvi <sup>c</sup>, László Rosta <sup>c</sup>, László Kovács <sup>d</sup>, Győző Garab <sup>d,\*\*</sup>

<sup>a</sup> IMFUFA, Department of Science, Systems and Models, Roskilde University, PO Box 260, DK-4000 Roskilde, Denmark

<sup>b</sup> Institut Laue-Langevin, BP 156, F-38042, Grenoble Cedex 9, France

<sup>c</sup> Research Institute for Solid State Physics and Optics, Hungarian Academy of Sciences, H-1525, Budapest, Hungary

<sup>d</sup> Institute of Plant Biology, Biological Research Centre, Hungarian Academy of Sciences, PO Box 521, H-6726, Szeged, Hungary

### ARTICLE INFO

#### Article history:

Received 28 October 2011

Received in revised form 30 December 2011

Accepted 20 January 2012

Available online 28 January 2012

#### Keywords:

Granum

Light-induced reorganization

Repeat distance

Small-angle neutron scattering (SANS)

Stroma thylakoid membrane

Transmembrane proton gradient

### ABSTRACT

The multilamellar organization of freshly isolated spinach and pea chloroplast thylakoid membranes was studied using small-angle neutron scattering. A broad peak at  $\sim 0.02 \text{ \AA}^{-1}$  is ascribed to diffraction from domains of ordered, unappressed stroma lamellae, revealing a repeat distance of  $294 \text{ \AA} \pm 7 \text{ \AA}$  in spinach and  $345 \text{ \AA} \pm 11 \text{ \AA}$  in pea. The peak position and hence the repeat distance of stroma lamellae is strongly dependent on the osmolarity and the ionic strength of the suspension medium, as demonstrated by varying the sorbitol and the  $\text{Mg}^{++}$ -concentration in the sample. For pea thylakoid membranes, we show that the repeat distance decreases when illuminating the sample with white light, in accordance with our earlier results on spinach, also regarding the observation that addition of an uncoupler prohibits the light-induced structural changes, a strong indication that these changes are driven by the transmembrane proton gradient. We show that the magnitude of the shrinkage is strongly dependent on light intensity and that the repeat distance characteristic of the dark state after illumination is different from the initial dark state. Prolonged strong illumination leads to irreversible changes and swelling as reflected in increased repeat distances. The observed reorganizations are discussed within the frames of the current structural models of the granum-stroma thylakoid membrane assembly and the regulatory mechanisms in response to variations in the environmental conditions *in vivo*. This article is part of a Special Issue entitled: Photosynthesis Research for Sustainability: from Natural to Artificial.

© 2012 Elsevier B.V. All rights reserved.

### 1. Introduction

In higher plants, the photosynthetic pigment–protein complexes are embedded in the thylakoid membranes, which are located in the chloroplast, and are surrounded by an aqueous matrix, the stroma. Electron microscopy has long since revealed that the thylakoid membrane is organized into an intricate structure differentiated into closely appressed (stacked) flattened vesicles, the granum thylakoids, and the non-appressed stroma lamellae interconnecting the grana [1–3]. In a scattering context, the stroma lamellae can be viewed as a loose regular stack of lamellae. The thylakoid membrane system is formed

from one continuous membrane, which encloses a contiguous single interior aqueous phase, the thylakoid lumen. Although our understanding of the self-assembly and some details of the membrane ultrastructure remain to be clarified, electron tomography data unequivocally reveal that not only the grana but also the stroma thylakoids are constituted of lamellar sheets [4–9] (and not narrow bridges between grana, as is erroneously depicted in some textbooks cf. [2]).

In accordance with the presence of the two morphologically distinct regions in the thylakoid membranes, the main protein complexes are laterally segregated: the ATP synthase and photosystem I (PSI), both having bulky stroma-exposed parts, are found in the non-appressed regions, i.e. in the stroma lamellae and the end membranes of the grana, while photosystem II (PSII) with light harvesting complex II (LHCII), which have limited protrusions to the stromal side, are predominantly situated in the appressed membranes of the grana [10,11] and the cytochrome  $b_6/f$  complex is distributed more or less evenly between the two regions. This membrane architecture is optimized such that the tight stacking of grana membranes with a large area to volume ratio increases the efficiency of light capturing

**Abbreviations:** LHCII, light harvesting complex II; PMS, phenazine methosulphate; PSI, photosystem I; PSII, photosystem II; SANS, Small-Angle Neutron Scattering; SAXS, Small-Angle X-ray Scattering

<sup>☆</sup> This article is part of a Special Issue entitled: Photosynthesis Research for Sustainability: from Natural to Artificial.

\* Corresponding author. Tel.: +45 4674 2607; fax: +45 4674 2030.

\*\* Corresponding author. Tel.: +36 62 433131; fax: +36 62 433434.

E-mail addresses: [Dorthe@ruc.dk](mailto:Dorthe@ruc.dk) (D. Posselt), [gyozo@brc.hu](mailto:gyozo@brc.hu) (G. Garab).

and warrants an overall high packing density of the membranes [2]. The segregation is also believed to play an important role in the ability of plants to adjust to environmental changes influencing the photosynthetic activity, e.g. changes in the illumination level requiring photosynthetic regulation with redistribution of light energy between the two laterally separated photosystems [11]. The thylakoid ultrastructure is both very stable and exhibits a high degree of flexibility in response to dynamically changing environmental conditions, as also evidenced by the results presented in this work.

Chloroplasts of higher plants are biconvex in shape with a length of a few micrometers. From electron microscopy it is known that the thylakoid membrane folded up inside the chloroplast typically has 40–60 cylindrical grana, each consisting of typically ~5–20 flattened vesicles (thylakoids) with diameters of ~3000–6000 Å [1,2,11]. The repeat distance,  $D_{\text{grana}}$  (Fig. 1) between units in the grana stack (i.e. the height of a granum thylakoid plus the height of the interthylakoid space across to the next granum vesicle) varies between 144 and 243 Å as cited from 17 different electron microscopy works on different plants in [11], with distances between 160 and 210 Å being most common. Recently, using cryoelectron tomography, the value of  $D_{\text{grana}}$  was found to be 157 Å in isolated intact spinach chloroplasts [8]. The repeat distance between the non-appressed stroma lamellae,  $D_{\text{stroma}}$  (Fig. 1) is considerably larger, typically by a factor of 2–3.3 [12,13]. Distances within the grana unit cell estimated from cryoelectron tomography are a lumen width of 45 Å and an interthylakoid distance of ~32 Å [8]. Allowing for a membrane thickness of ~40 Å, gives a total  $D_{\text{grana}}$  of 157 Å (each repeating unit cell contains two bilayers), while data from small-angle X-ray scattering allow for a somewhat larger lumen width and thus a larger repeat distance [14–16]. In our analysis of neutron scattering data, we view the thylakoid membrane system as two diffracting systems (grana thylakoids resp. stroma lamellae) each with order in one dimension, an idea which holds independently of the exact three dimensional organization of the membranes.

The characteristic length scales of the thylakoid membrane are in the range of  $10^1$ – $10^3$  Å and thus small-angle scattering techniques [17,18] are well suited to study the ultrastructure of this multilamellar membrane system. In comparison with electron

microscopy, small-angle scattering of either neutrons or X-rays has the advantage that there is no need for any staining or fixation of the system under investigation, i.e. the dynamic response of the system can be explored. Complementary to electron microscopy, which delivers direct information about the local structure, data from small-angle scattering are averaged over a macroscopic sample volume; however, the information is given in reciprocal space and interpretation requires implementation of modeling of various degrees of sophistication.

Early small-angle X-ray scattering (SAXS) works on chloroplasts used samples which were stained with  $\text{OsO}_4$  [19] or dried in various ways [20,21]. In addition, conclusions based on studies carried out before the Singer–Nicholson model of the bilayer membrane [22] was generally accepted, are to various extents misleading due to membrane models basically constructed as stacked layers of lipids, proteins and chlorophylls. SAXS investigations of spinach chloroplasts in suspension under physiological conditions and aligned in a magnetic field [23] demonstrated that magnesium plays a role in the stacking interaction between membranes in a grana stack. SAXS data of osmotically dehydrated spinach thylakoids were analyzed using a finite paracrystalline lattice model and repeat distances between 145 and 230 Å depending on osmotic pressure and salt concentration were found. All SAXS work cited above ignores the presence of stroma membranes in the thylakoids and interprets results exclusively in terms of the periodicity of the stacked granum thylakoid membranes. We have previously investigated spinach thylakoids in suspension using SAXS and analyzing the data using a Gaussian one-dimensional model of the electron density distribution including both grana and stroma membranes [14] and have simulated the scattering profile [15]. In both cases the results showed the necessity of including stroma membranes in the data analysis.

While electron density differences are giving the contrast in SAXS, the contrast in small-angle neutron scattering (SANS) is provided by the different scattering length densities of the membrane components. These scattering length densities are determined by the scattering lengths of the component atoms, which vary in a random fashion throughout the periodic table and also between different isotopes of the same element. SANS gives the unique possibility of

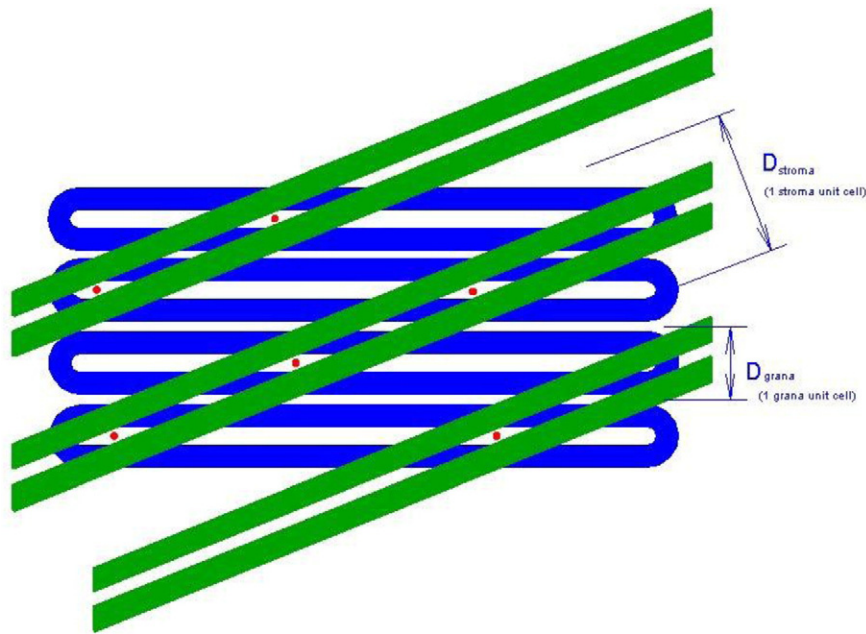


**Fig. 1.** Schematic drawing of the topology of the membrane system. The repeat distances of the grana stack,  $D_{\text{grana}}$ , and for the stroma lamellae,  $D_{\text{stroma}}$ , are indicated in the figure. The thick green and blue lines represent the lipid bilayer membranes of the stroma lamellae and grana thylakoids, respectively. The red dots indicate the fusions between the grana and the stroma lamellae, ensuring the continuity of the internal lumenal space. The stroma lamellae are tilted with respect to the grana membranes, in accordance with the helical arrangement of the stroma lamellae around the granum.

contrast variation by substituting hydrogen with deuterium, in the most straightforward way by simply mixing H<sub>2</sub>O and D<sub>2</sub>O in the suspending medium. Sadler and Worcester [24] studied oriented thylakoid membranes isolated from algae and spinach with SANS. Orientation was done either by controlled evaporation (algae) or by magnetic orientation of the membranes in aqueous suspensions (spinach). The 3D organization of the thylakoid membranes is different for algae and spinach, particularly at the relevant length scales studied here, i.e. the characteristic small-angle scattering is different for the two kinds of sample [25]. For spinach chloroplasts in suspension and aligned in a magnetic field, a peak of scattered intensity corresponding to a Bragg distance of ~250 Å was observed [24]. This repeat distance was interpreted to originate from grana. The peak was best resolved with the chloroplasts suspended in pure D<sub>2</sub>O, while the contrast was minimal in 30% (v/v) D<sub>2</sub>O in H<sub>2</sub>O.

The SAXS/SANS results for the structure of thylakoid membranes are very dependent on the source of the thylakoid membrane studied, the detailed sample preparation and the composition of the suspension medium. The observed profiles also depend on a possible orientation procedure, which can be used to enhance the characteristic features of the scattering. In this work, we show that, in contrast to previous interpretations, the main SANS peak from freshly isolated, magnetically aligned spinach and pea thylakoid membranes under physiological conditions, arises from the regular arrangement of the stroma lamellae. In addition, we demonstrate how SANS reflects reorganizations in the ultrastructure when the system is subjected to physico-chemical changes in the environment, such as variations in the osmolarity or the ionic strength of the suspension medium. These variations in  $D_{\text{stroma}}$  can be rationalized by taking into account the macroorganization of the complexes in the granum-stroma thylakoid membrane assembly with its intricately organized continuum membrane system. We also show how SANS can be used for studying the light-induced reorganizations in the membrane ultrastructure, structural changes which appear to be of fundamental importance during photosynthesis.

## 2. Materials and methods

### 2.1. Sample preparation

Thylakoid membranes were freshly isolated either from market spinach (Budapest and ILL measurements) or young pea leaves grown in-situ (PSI measurements). The typical procedure for isolation of thylakoid membranes is described below and in [14,26], however details regarding e.g. salt concentration and exact centrifugation parameters (time and acceleration) varied a little, but this is without significance for the structure. The leaves were kept in the dark on ice or in the fridge before isolation and all equipment used was kept on ice. The leaves were homogenized using a blender in a medium containing 0.4 M sorbitol, 5 mM MgCl<sub>2</sub>, 5 mM KCl and 20 mM tricine, pH 7.6. In order to remove debris, the suspension was filtered through 8 layers of cheesecloth and centrifuged for 2 min at 200×g (spinach) or 15 s at 3000×g (pea). The supernatant was recovered and centrifuged for 3 min at 4500×g. The pellet was carefully resuspended using a soft brush. To remove the envelope membranes of chloroplasts the suspension was then subjected to a brief osmotic shock by resuspending the pellet in a hypotonic medium containing 5 mM MgCl<sub>2</sub>, 5 mM KCl and 20 mM tricine, pH 7.6 and centrifuged again for 4 min at 5000×g. The resulting pellet was resuspended in a buffer containing 0.4 M sorbitol, 5 mM MgCl<sub>2</sub>, 5 mM KCl and 20 mM tricine, at various D<sub>2</sub>O to H<sub>2</sub>O ratios as specified in the text. The spinach samples measured in Budapest were suspended in a 100% D<sub>2</sub>O (pD 8.0) medium containing deuterated glucose instead of sorbitol, while the pea samples at the PSI used for illumination studies, were suspended in a 100% D<sub>2</sub>O medium (pD 8.0) containing deuterated glucose (98% 7D-glucose). In addition to the salts and buffer mentioned

above 100 μM PMS (phenazine methosulphate) was added to these samples. At the ILL the spinach samples were measured in either pure H<sub>2</sub>O, 40% D<sub>2</sub>O/60% H<sub>2</sub>O or in pure D<sub>2</sub>O with 20 mM tricine, 10 mM KCl and varying amounts of non-deuterated sorbitol, and MgCl<sub>2</sub>. (The SANS protein contrast is zero for 40% D<sub>2</sub>O). For SANS measurements, the chlorophyll content of the samples was adjusted to approx. 1–4 mg/ml, with the actual value determined spectrophotometrically [27] and the samples were filled in 1 mm or 2 mm quartz cuvettes (Hellma 110-QS). Transmission Electron Microscopy (TEM) on isolated pea thylakoid membranes, showed the expected structure with  $D_{\text{grana}} = 164 \text{ Å} \pm 25 \text{ Å}$  and  $8 \pm 3$  grana thylakoids per stack in a standard suspension with 0.4 M sorbitol, while suspension in 2.0 M sorbitol medium resulted in a lower value of  $D_{\text{grana}} = 159 \text{ Å} \pm 18 \text{ Å}$ , with  $9 \pm 5$  granum thylakoid membranes per stack (courtesy of Alexander Schulz, Center for Advanced Bioimaging (CAB) Denmark, University of Copenhagen and Kasper Swiatek, RUC). The samples were kept at 4 °C in the dark after isolation and resuspension in the relevant reaction medium and used within at most 8 h. During this time-period no changes in the SANS peak positions were observed and similarly no changes were observed in the photosynthetic activity as measured by chlorophyll-a fluorescence induction using a PAM 101 chlorophyll fluorometer (WALZ, Effeltrich, Germany).

### 2.2. Small-angle neutron scattering

Small-angle neutron scattering (SANS) experiments were carried out at the “Yellow Submarine” SANS instrument of the Budapest Neutron Centre (BNC, Budapest, Hungary), at the SANS-II station of the Paul Scherrer Institute (PSI, Villach, Switzerland) and at the D22 beamline of the Institut Laue-Langevin (ILL) in Grenoble. All data shown in this paper are from the PSI and the ILL, however we will also refer to results and experiences from the BNC. The neutron beam at all three facilities were monochromatized using a mechanical velocity selector. The detector of BNC was a 64×64 pixel, BF<sub>3</sub> gas filled, two dimensional multiwire position sensitive detector with a pixel size of 1 cm×1 cm. The detector at PSI was a two-dimensional multiwire position sensitive <sup>3</sup>He detector with 128×128 pixels, each pixel size being 0.5 cm×0.5 cm. Three different instrument settings were used covering the q-range between 0.0036 Å<sup>-1</sup> and 0.25 Å<sup>-1</sup>: sample-to-detector distances of 1 m and 5 m with a wavelength of 6.37 Å and collimation distances of 2 m and 6 m, respectively, and a sample-to-detector distance of 6 m with a wavelength of 10.6 Å and a collimation distance of 4 m. In all cases  $\Delta\lambda/\lambda \sim 18\%$ , and 16 mm diameter pinholes in the collimation section and 8 mm diameter pinhole before the sample were used. Most samples were only measured at the 6 m/10.6 Å setting since the peak of interest is in the q-range covered by this setting. At the ILL the detector was a 128×128 pixel <sup>3</sup>He multidetector, with a pixel size of 0.8 cm×0.8 cm. Two different instrument settings were used covering the q-range between 0.008 and 0.2 Å<sup>-1</sup>: sample-to-detector distances of 2.45 m and 8 m with neutron wavelength of 6 Å,  $\Delta\lambda/\lambda \sim 10\%$  and collimation distances of 2.8 m and 8 m respectively, with a 10 mm×6.5 mm slit in front of the sample. The samples were aligned in a magnetic field of ~1 T using an electromagnet in Budapest and at the ILL, while permanent magnets (~0.4 T) were used at the PSI. In the absence of an external magnetic field, a relatively weak ring of scattering was observed at the q-value corresponding to the peak position for the oriented sample – showing that the magnetic field does not affect the repeat distances. The grana membranes' normals tend to align parallel to the applied field [28]. The aligning effect is caused by an anisotropy in the diamagnetic susceptibility of thylakoid constituents, in particular of the light harvesting complexes [29]. Samples were thermostated at 15 °C or 20 °C or measured at room temperature. Typical measuring times were 30–45 min at the BNC, 15 min at the PSI and 5 min at the ILL.

### 2.3. Data reduction and analysis

The PSI (pea) data were corrected in order to ensure equidistance of the pixel grid and the data were normalized to the incoming neutron flux. A water sample was used for correction of detector efficiency. Background (scattering from the buffer and the sample holder) and electronic noise were subtracted taking transmissions into account. The data were radially averaged around the center of the direct beam in 75° wide sectors (see Fig. 4). This width was found to minimize the standard deviation in peak position. The data analysis was done using the Graphical Reduction and Analysis SANS Program for Matlab (developed by Charles Dewhurst, ILL). Peak positions,  $q^*$ , were found from the radially averaged curves by fitting a Gaussian to a (asymmetrical) range of points around the peak. The repeat distance or Bragg spacing,  $D$ , of the system was calculated as  $2\pi/q^*$ . The ILL (spinach) data were analyzed in the same manner, except that the width of the sectors for averaging was 45°, in accordance with the aligning field being stronger. For the determination of peak positions, a sum of a Gaussian (Bragg peak) and a power function (polydispersity) were fitted to the data. If the sample is regarded as composed of identical unit cells placed on an underlying lattice, i.e. the grana cylinders and the stroma lamellae are each composed of flattened vesicles, placed with regular intervals, the scattered intensity  $I$ , as a function of scattering vector  $\vec{q}$ , is given by  $I(\vec{q}) \propto |F(\vec{q})|^2 \cdot S(\vec{q})$ , where the form factor,  $F(\vec{q})$ , squared is proportional to the scattering from an individual unit cell, and the structure factor,  $S(\vec{q})$ , describes the scattering arising from the periodicity of the underlying lattice on which the unit cells are placed. In the present case, there is a form factor and a structure factor describing the grana stack and a different form factor and structure factor for the periodically spaced (non-apressed) stroma lamellae.

### 2.4. Illumination

For illumination of pea samples during the measurements at the PSI, an optical fiber was inserted through a flange in the vacuum sample chamber and connected to a lamp with adjustable spectral and diaphragm settings (Schott lamp KL 1500). The intensity of the lamp was measured using a calibrated LI-190SZ quantum sensor, which has a linear response in the PAR range (Photosynthetically Active Radiation range, 400–700 nm). Two illumination schemes with white light were used: short-cycle illumination and continuous illumination. With short cycles, typically 4 min of light was followed by 4 min of darkness in repeated cycles and data collection took place during the last 3 min. With the continuous illumination scheme, light was turned on and data collection started after 1 min in the light and continued until sufficient statistics was obtained, usually within 15 min. No significant differences were found between the two protocols, thus most of the illumination data were collected with continuous illumination.

## 3. Results

### 3.1. Dark adapted magnetically aligned thylakoid membranes

The repeat distance average and standard deviation from 12 freshly prepared, dark adapted pea samples from 5 different isolations, are  $345 \text{ \AA} \pm 11 \text{ \AA}$ , with all values in the range of 320–355 Å. The values for spinach are somewhat lower, in the range of 285–300 Å, with an average of  $294 \text{ \AA} \pm 7 \text{ \AA}$  from 4 samples. These values are much too high to be attributed to Bragg diffraction from  $D_{\text{grana}}$  (cf. data in Introduction). However, as shown in Fig. 1, the stroma lamellae also form a regular lattice albeit with more disorder than the grana stacks [5,8,9]. With the grana stack normal parallel to the applied field, diffraction from the stroma lamellae is expected to occur at an angle of

typically  $\sim 10^\circ$ – $22^\circ$  [5,8] with respect to the vertical  $q_z$ -axis. However, on the backside of the grana stack, the stroma lamellae are oriented at an angle of  $\sim -22^\circ$ – $-10^\circ$  and, due to disorder inherent in the biological system and due to non-perfect alignment, there is a smearing giving the rather broad diffraction peak observed. No higher order stroma lamellar peaks are observed. As concerns the (quasi-)helical structure of the stroma thylakoids around the grana, it would be expected to give rise to a characteristic helical diffraction pattern [30] which, however, cannot be discerned. For the non-ideal thylakoid structure many factors contribute to smearing of the ideal scattering pattern (stroma lamellae losing imposed helical order further away from the grana stack, other types of inherent disorder and imperfections of the grana stacks; also, contribution of form factor scattering is neglected). The helical structure, and the tilt angle of the membranes would give rise to only a minor increase in the calculated repeat distances [31]. Hence, the simple interpretation in terms of a first order Bragg peak from parallel membrane sheets appears to be satisfactory. Diffraction from the grana stack is expected in the range of  $0.026 \text{ \AA}^{-1}$ – $0.044 \text{ \AA}^{-1}$  [11]. We do observe a broad peak at high  $q$ -values, but around  $0.075 \text{ \AA}^{-1}$ , both for pea and for spinach, but there is no peak in the expected region. The  $0.075 \text{ \AA}^{-1}$  peak might be form factor related or alternatively a second order peak corresponding to the grana stack order ( $2\pi/0.075 \text{ \AA}^{-1} = 84 \text{ \AA}$ , i.e. a grana stack repeat distance of  $2 \cdot 84 \text{ \AA} = 168 \text{ \AA}$ , which is realistic). If the  $0.075 \text{ \AA}^{-1}$  feature is a second order grana peak, the question naturally arises why no first order peak is seen, one possible explanation being that such a peak might coincide with a form factor minimum. This issue will be discussed in a separate paper (in preparation).

### 3.2. Variations of the osmotic pressure

Spinach thylakoid membranes suspended in an extreme hypotonic medium (standard medium without sorbitol) can only be aligned to some extent in a relatively strong magnetic field. Inspection of isolated pea thylakoids in a hypotonic medium in the light microscope shows that the structure is highly swollen with formation of clusters of vesicles (not shown). The standard suspension medium with 0.4 M osmoticum (in casu sorbitol) is close to the isotonic conditions. We have measured a series of dark adapted spinach thylakoid membranes suspended in a medium with 10 mM  $\text{MgCl}_2$ , 10 mM KCl, 20 mM tricine in 40%  $\text{D}_2\text{O}$  and varying amounts of sorbitol: 0, 0.1, 0.4, 1 and 2 M (Fig. 2). All curves, except for the sample with no sorbitol, show a pronounced peak with the peak position and intensity dependent on the amount of sorbitol in the suspension medium. The sample without sorbitol shows a shoulder rather than a fully developed peak. The contrast between the aqueous phase (buffer solution) and the stroma lamellae decreases with increasing sorbitol content explaining the decreasing peak intensity. The incoherent background due to scattering from hydrogen is increasing with

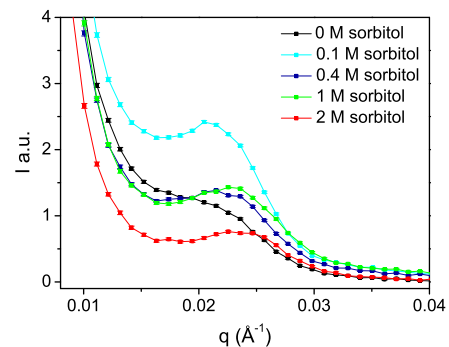


**Fig. 2.** SANS curves from isolated spinach thylakoid membranes suspended in a medium containing 10 mM  $\text{MgCl}_2$ , 10 mM KCl, 20 mM tricine (pH 7.6) in 40%  $\text{D}_2\text{O}$  and different amounts of sorbitol: 0, 0.1, 0.4, 1 and 2 M, as indicated.

increasing sorbitol content as observed at high  $q$ . The peak position is increasing with increasing amount of sorbitol, consistent with the expected shrinkage of the system with increasing osmotic pressure.  $D_{\text{stroma}}$  for the spinach sample at isotonic conditions is  $286 \text{ \AA} \pm 1 \text{ \AA}$ , while at hypertonic conditions the system shrinks to  $277 \text{ \AA} \pm 1 \text{ \AA}$  (1 M sorbitol) and  $269 \text{ \AA} \pm 1 \text{ \AA}$  (2 M sorbitol). At hypotonic conditions the system swells to  $297 \text{ \AA} \pm 1 \text{ \AA}$  (0.1 M sorbitol) and  $307 \text{ \AA} \pm 1 \text{ \AA}$  (no sorbitol) (the results are compiled in Table 1). The repeat distances found are independent of the  $D_2O/H_2O$  ratio as confirmed by control measurements in pure  $D_2O$  and pure  $H_2O$ .

### 3.3. Variations of the concentration of magnesium ions

It is well documented that stacking and unstacking of grana is controlled by the presence of cations [32]. The stromal side of the thylakoid vesicles are negatively charged such that there is an electrostatic repulsion between adjacent membrane surfaces. The negative charges are mainly due to exposed protein surfaces [33] but the contribution of negatively charged lipids also plays a significant role. The lipid composition in higher plant thylakoid membranes is ~50 mol% monogalactosyl diacylglycerol, 30 ~mol% digalactosyl diacylglycerol, ~5–12 mol% sulphoquinovosyl diacylglycerol and ~5–12 mol% phosphatidyl glycerol [34], where the last two are acidic, i.e. negatively charged at physiological pH values. In order to keep the tightly stacked structure of the grana, the Coulomb interaction between opposing membranes has to be screened by the presence of cations, typically  $Mg^{++}$ . Changes in the grana stacking are expected to influence also the stroma repeat distance, both because similar interactions, albeit to a lesser extent, are present between stroma membranes, but also as a result of the grana and stroma lamellae being physically attached to each other. We have measured SANS for spinach thylakoids suspended in low osmolarity medium (0.1 M sorbitol, 20 mM tricine, 10 mM KCl in 40%  $D_2O$ ) with respectively low concentration of  $MgCl_2$  (1 mM) and high concentration of  $MgCl_2$  (10 mM) and similarly for a high osmolarity medium (1 M sorbitol, 20 mM tricine, 10 mM KCl in 40%  $D_2O$  with respectively 1 mM and 10 mM  $MgCl_2$ ) – see Fig. 3 and Table 1. A clear shift in the peak position,  $q^*$ , towards lower values, i.e. loosening of the stacking ( $D = 2\pi/q^*$ ), for lower amounts of  $Mg^{++}$  is seen. For high osmolarity, the spinach stroma repeat distance changes from 277 to 317  $\text{\AA}$  (14% increase) and for low osmolarity from 297  $\text{\AA}$  to 332  $\text{\AA}$  (12% increase) when the amount of  $Mg^{++}$  is lowered from 10 mM to 1 mM.

### 3.4. Illumination

Irreversible structural changes were observed to occur when spinach thylakoid membranes suspended in 0.4 M sorbitol, 5 mM  $MgCl_2$ ,

**Table 1**

The effect of varying osmolarity and ionic strength on the stroma lamellar repeat distance of isolated spinach thylakoid membranes. The data corresponds to the data in Figs. 2 and 3. All suspending media contain 10 mM KCl and 20 mM Tricine in addition to Sorbitol and  $MgCl_2$  with concentrations as given in the table.

40% $D_2O$		Peak position ( $10^{-2} \text{ \AA}^{-1}$ )	Repeat distance ( $\text{\AA}$ )
Sorbitol (M)			
10 mM $MgCl_2$	0	$2.04 \pm 0.01$	$307 \pm 2$
10 mM $MgCl_2$	0.1	$2.12 \pm 0.01$	$297 \pm 1$
10 mM $MgCl_2$	0.4	$2.20 \pm 0.01$	$286 \pm 1$
10 mM $MgCl_2$	1	$2.27 \pm 0.01$	$277 \pm 1$
10 mM $MgCl_2$	2	$2.34 \pm 0.01$	$269 \pm 1$
$MgCl_2$ (mM)			
0.1 M sorbitol	1	$1.89 \pm 0.01$	$332 \pm 1$
0.1 M sorbitol	10	$2.12 \pm 0.01$	$297 \pm 1$
1 M sorbitol	1	$1.99 \pm 0.01$	$317 \pm 2$
1 M sorbitol	10	$2.27 \pm 0.01$	$277 \pm 1$

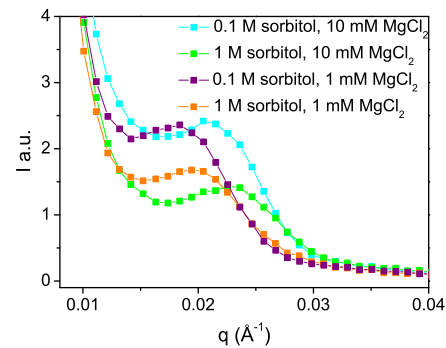


**Fig. 3.** SANS curves from isolated spinach thylakoid membranes suspended in a medium containing 0.1 M sorbitol, 10 mM KCl and 20 mM tricine (pH 7.6) in 40%  $D_2O$  and 1 mM resp. 10 mM  $MgCl_2$  and in a medium containing 1 M sorbitol, 10 mM KCl and 20 mM tricine in 40%  $D_2O$  and 1 mM resp. 10 mM  $MgCl_2$ , as indicated.

5 mM KCl and 20 mM tricine in the absence of electron donors or acceptors, were pre-illuminated with white light of  $\sim 2500 \mu\text{mol photons m}^{-2} \text{ s}^{-1}$  for 15 min. During pre-illumination the sample was thermostated at 15  $^{\circ}\text{C}$  in a water bath. The pre-illuminated membranes show a shift of peak position corresponding to a ~8% increase in  $D_{\text{stroma}}$  in the standard isotonic suspension medium and a ~4% increase in high osmolarity suspension medium (data not shown).

Freshly isolated pea thylakoid membranes suspended in media containing PMS, which facilitates photosystem I cyclic electron transport, were illuminated in-situ, during SANS measurements. The light intensity used was not higher than  $2000 \mu\text{mol photons m}^{-2} \text{ s}^{-1}$  and under these conditions the structural changes observed were largely reversible. For all illuminated samples a very clear shift in the peak position towards larger  $q$  is observed directly in the 2D images (Fig. 4). When turning the light off, the position of the peak returns to smaller  $q$ , i.e. a light-induced reversible shrinkage is observed – as reported by us earlier for stroma lamellae of isolated spinach thylakoid membranes [25], in contrast to the swelling caused by irreversible pre-illumination. The light-induced reversible shrinkage is also clearly seen on the sectorially averaged  $I(q)$  curves (Fig. 4), where it is also evident that illumination causes smearing of the peak.

An important characteristic feature for these measurements is that the first dark adapted curve is always different in intensity and shape from the dark adapted curves after the sample has been illuminated. This is clearly seen in Fig. 5, where the light intensity and the duration of illumination have been varied. The black curve is the initial dark adapted sample, which is very different from the other curves which fall into two groups: illuminated samples and the following dark adapted states. Fig. 5b shows the repeat distance for the different cases and it is seen that the system cycles between two states – an illuminated state with repeat distance around 280  $\text{\AA}$  ( $q^* = 0.0224 \text{ \AA}^{-1}$ ) and a dark state with repeat distance around 310  $\text{\AA}$  ( $q^* = 0.0203 \text{ \AA}^{-1}$ ), i.e. illumination causes a shrinkage of ~10%. The same overall picture emerges from measurements on more than 10 different samples of isolated pea thylakoid membranes from eight different batches, although not always so clear cut. There is a strong dependence of the stroma repeat distance on the light intensity (Fig. 6a – note that each point represents a different sample) in the illuminated state, the repeat distance decreasing systematically from 355  $\text{\AA}$  ( $q^* = 0.0177 \text{ \AA}^{-1}$ ) in the dark state to 271  $\text{\AA}$  ( $q^* = 0.0232 \text{ \AA}^{-1}$ ) in the state illuminated with  $1000 \mu\text{mol photons m}^{-2} \text{ s}^{-1}$ . Fig. 6b shows the difference in repeat distance between the original dark adapted sample and the first illuminated sample in each case as a function of light intensity and there is a strong increase in this change from ~20  $\text{\AA}$  with  $50 \mu\text{mol photons m}^{-2} \text{ s}^{-1}$  to 85  $\text{\AA}$  for  $1000 \mu\text{mol photons m}^{-2} \text{ s}^{-1}$ . The  $2000 \mu\text{mol photons m}^{-2} \text{ s}^{-1}$  data point is left out from the comparison in Fig. 6b and c due to an

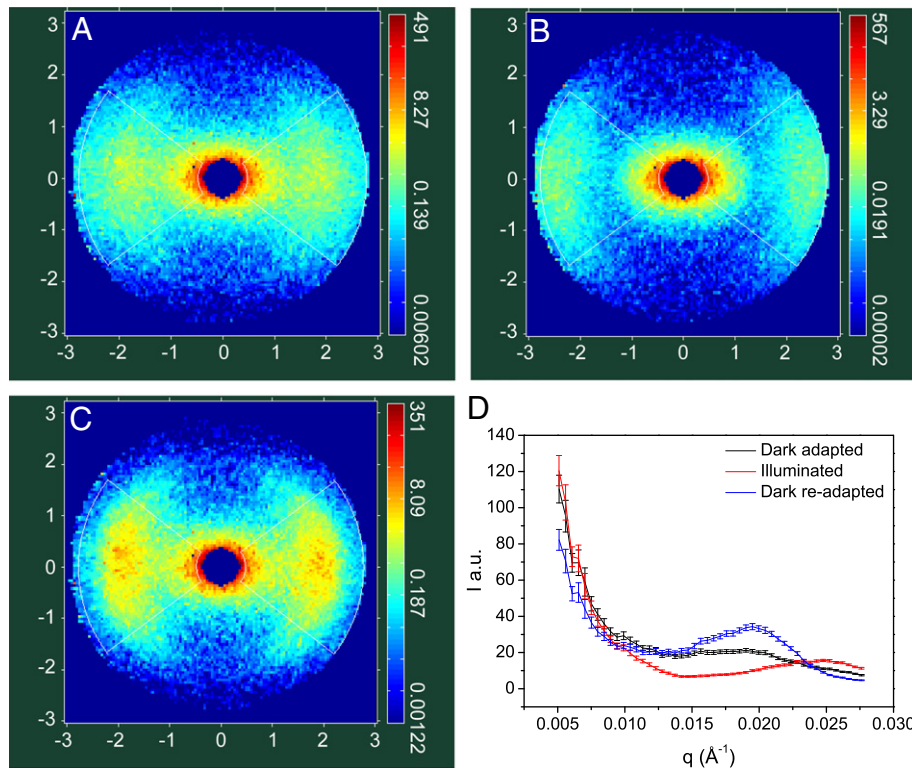


**Fig. 4.** 2D (A–C) and 1D (D) scattering profiles of isolated pea thylakoid membranes. (A) Dark adapted sample. (B) Illuminated sample, white light of  $1000 \mu\text{mol photons m}^{-2} \text{s}^{-1}$  for 15 min. (C) Dark re-adapted sample (after 45 min of illumination) (D) Corresponding radial sector averages of the scattering intensity as a function of  $q$  ( $75^\circ$  sectors shown on the 2D images).

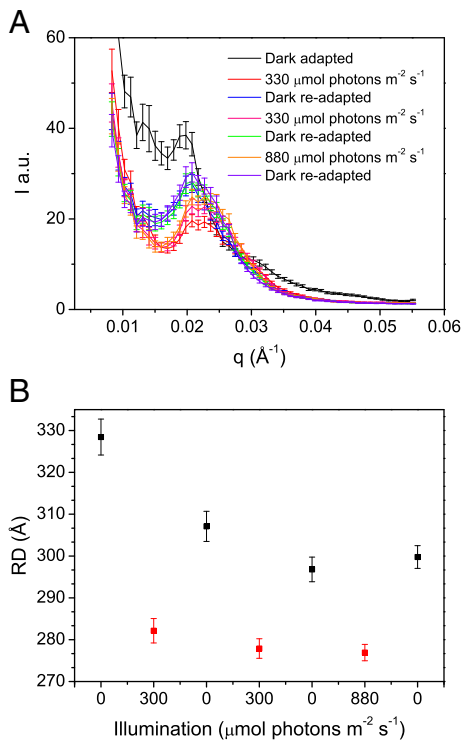


**Fig. 5.** Effect of illumination and dark re-adaptation on the SANS of isolated pea thylakoid membranes. Consecutive light/dark experiments: first illumination, 30 min; subsequent illuminations and dark re-adaptations, 10 min each. (A) radially averaged data; (B) The repeat distance corresponding to the peak position for each curve: black data points are dark measurements ( $0 \mu\text{mol photons m}^{-2} \text{s}^{-1}$ ) and red is illuminated using light intensities as indicated.

ill-defined peak-shape for the first dark sample for this particular case. It is generally observed that there is a difference between the repeat distance of the initial dark adapted sample and the first dark re-adapted sample. Fig. 6c shows that the difference between these two values increases with the pre-illumination intensity. Some of our data indicate that processes with different time scales are at play, i.e. longer illumination times ( $>30$  min) seem to show indications of a different behavior. In a sample without PMS added, the behavior in the first 15 min illumination cycle follows the general pattern, but a second illumination with  $1000 \mu\text{mol photons m}^{-2} \text{s}^{-1}$  does *not* significantly change the scattering pattern in contrast to our general observations when PMS is added to the suspension medium. In the presence of  $5 \text{ mM NH}_4\text{Cl}$ , an uncoupler, which eliminates the proton gradient across the thylakoid membrane [35], the peak in the curves is not as pronounced as for samples without  $\text{NH}_4\text{Cl}$  and illumination does not significantly change the scattering curves (data not shown). While the effect of this uncoupler on the scattering profile is not understood and requires further investigation, the inhibition of the light-induced changes is a further clear indication that the observed structural changes are related to the basic photosynthetic process. This is in accordance with our data showing a similar effect when adding the uncoupler nigericin [25] and confirms the role of the transmembrane proton gradient in driving the reorganization in the lamellar order of the stroma thylakoid membranes.

#### 4. Discussion

Our interpretation of the SANS curves for pea and spinach thylakoids is based on the observation that the grana stack and the stroma lamellae each constitute a long-range ordered system with one-dimensional periodicity along their membrane normals. The basic units piled on top of each other are bilayer–lumen–bilayer–interthylakoidal space in the grana and bilayer–lumen–bilayer–stroma aqueous phase in the case of stroma lamellae.

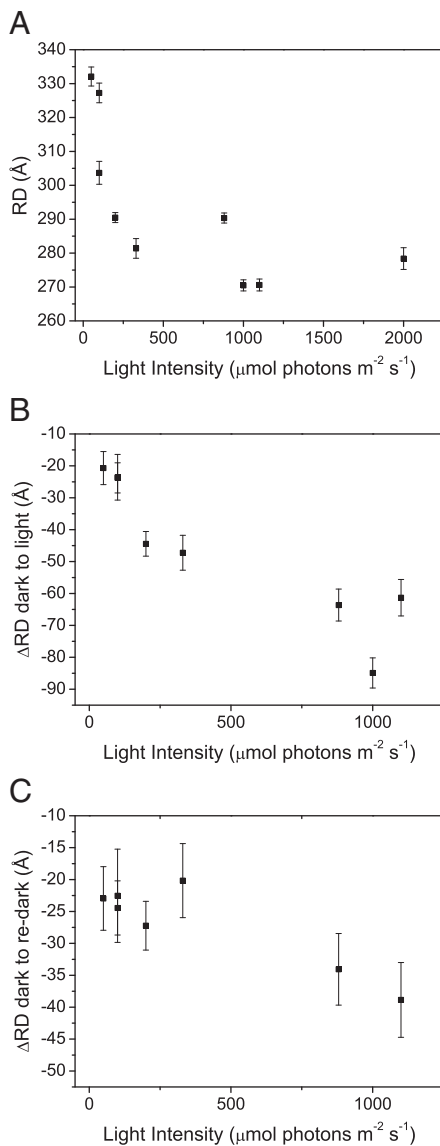


**Fig. 6.** Variations in the stroma lamellar repeat distance of isolated pea thylakoid membranes as a function of illumination intensity. (A) Dependence of the repeat distance on the intensity of illumination — each data point were obtained on a different sample. (B) The light-induced change in the repeat distance relative to the first dark adapted state as a function of the illumination intensity. (C) The difference between the repeat distances of the initial dark and the first dark re-adapted states as a function of the intensity of the illumination.

Previous analyses of SANS curves cited in the Introduction, have focused exclusively on the grana stack, while based on electron microscopy data from the literature and from our own samples, we conclude that the SANS peak at  $\sim 0.02 \text{ \AA}^{-1}$  originates from Bragg diffraction from the stroma lamellae. The stroma lamellae repeat distance for pea, measured in 100% D<sub>2</sub>O is  $\sim 12\%$  larger than for spinach, measured in 40% D<sub>2</sub>O, while the variation for a given species under the same conditions (i.e. the biological variability from batch to batch) is  $\sim 5\%$  with some more extreme ( $\sim 10\%$ ) cases occasionally occurring. The SANS contrast is different in suspension media with different D<sub>2</sub>O content. Control experiments confirm, however, that there is a relatively large difference between the repeat distances of the two species, independent of the contrast, i.e. the D<sub>2</sub>O/H<sub>2</sub>O ratio in the sample.

There is some discussion in the literature as to the detailed three dimensional organization of the thylakoid membranes [4–9]. The helical model for the membrane ultrastructure of granal chloroplasts

was first formulated by Paolillo in 1970 [36]. In this model, the stroma lamellae are wound around the central grana stack in a right handed helix tilted  $\sim 20^\circ$  with respect to the grana stack normal and attached to the grana through slits placed regularly around the rims of the flattened vesicles constituting the grana stack. The basic features of this model have been confirmed by recent electron tomography data — albeit the periodicity of the helical organization and thus also the regularity of the junctions are far less expressed than expected, and also the tilt angles appear to vary [3,5,9]. In the alternative model [4], the pairwise organization model, the stroma membranes are perpendicular to the grana normal and the stroma membranes bifurcate into two granum membranes: in each granum ‘vesicle’ unit, part of the top membrane layer bends upward and fuses with the membrane layer above it, whereas the bottom membrane bends downward at the opposite side and fuses with the membrane below thus ensuring the fully connected topology of the thylakoids. The units of paired grana are rotated relative to each other around the axis of the granum cylinder. There is strong evidence in the literature in favor of the quasi-helical model [3,9], however, our interpretation of the thylakoid SANS curves are valid for both models.

Membrane inserted and membrane bound protein complexes with polypeptides protruding from the thylakoid membrane put a limit to how close membranes can approach each other, i.e. there is a lower limit to the width of the lumen resp. the interthylakoidal space in the grana and to the distance between the stroma lamellae. Adjacent membranes in the grana contain PSII and LHCII, which are flat and protrude no more than 10–20 Å beyond the membrane surface in the interthylakoidal space [37]. This allows for a tight packing of the appressed membranes to be held together by electrostatic and van der Waals forces [38,39]. In contrast, the distance between the stroma lamellae must be considerably larger, due to the presence of PSI and the ATP synthase in these membrane sections, since the ATP synthase protrudes  $\sim 140 \text{ \AA}$  from the membrane on the stromal side [40], while PSI protrudes about 50 Å to the same side [37]. Allowing 40 Å for each membrane and 45 Å for the lumen [8], a minimum stroma repeat distance of 265 Å is found, however this distance assumes ATP synthase to reach fully across the space available, with no protruding unit on the opposite side, so somewhat larger values are not unrealistic.

Reorganizations in the ultrastructure, induced by physico-chemical factors, such as the ionic strength and osmolarity of the suspending medium have been thoroughly documented with the aid of electron microscopy [41]. SAXS investigations on thylakoid membranes aligned in a magnetic field also demonstrated that magnesium and sucrose or sorbitol play important roles concerning the structure of the thylakoid membranes [15,23]. Our data confirm that osmolarity influences the ultrastructure — in isotonic medium the repeat distance for spinach thylakoids was 286 Å, which corresponds to the distance expected based on electron tomography [8]. Increasing the osmolarity results in shrinkage of the system as expected — the system shrinks by up to 6% This value can be compared to our TEM data from which we know that the pea grana repeat distance shrinks 3% when increasing the sorbitol concentration from 0.4 M to 2 M. Likewise the stroma repeat distance increases by 7% with no osmoticum present compared to the control sample. The shrinkage is expected to take place in the lumen of the stroma thylakoid membranes (as well as in the luminal phases of the grana), while the distance between pairs of stroma lamellae is mainly dependent on geometry, i.e. if the grana stack shrinks or swells, the adjoined stroma lamellae are moved, too (cf. Fig. 1). It should be noted that there is a limit to the shrinkage of the luminal spaces during the described process, due to the proteins protruding from the membranes rather far into the luminal spaces. The structural changes induced by changing the concentration of osmoticum can be reversible as previously shown on the diatom *Phaeodactylum tricornutum* [42].

Our data are consistent with the well-known result, that by varying the amount of Mg<sup>++</sup> in the system, the membrane–membrane

interactions can be manipulated [32]. We expect the main effect of Coulomb screening to take place between the tightly appressed grana stacks. The adjoined stroma lamellae, however, adjust accordingly as was the case with the variation of osmolarity. Somewhat surprisingly, the effect of varying the amount of cations is larger than the effect of varying the amount of osmoticum, suggesting that grana, and stacking in particular, can play an important role also in the stroma lamellar reorganizations. We have tested the reversibility of these data at the BNC by measuring spinach thylakoid membranes in a suspension medium with a  $Mg^{++}$  concentration of 10 mM, afterwards transferring this sample to a medium with 1 mM  $Mg^{++}$  and finally back to the 10 mM  $Mg^{++}$  medium. The data show good reversibility with  $D_{stroma}$  for the first sample being equal to 299 Å ( $q^* = 0.021 \text{ \AA}^{-1}$ ), increasing to 328 Å ( $q^* = 0.0192 \text{ \AA}^{-1}$ ) in the low  $Mg^{++}$  concentration sample and finally decreasing to 304 Å ( $q^* = 0.021 \text{ \AA}^{-1}$ ).

Our observation that the system swells irreversibly when illuminated with high-intensity white light is consistent with a certain degree of disorganization of the membrane ultrastructure as is observed with light- and X-ray microscopy [14]. Fundamental investigations of light-induced reversible reorganizations in the thylakoid membrane ultrastructure were carried out by Murakami and Packer [43]. Using electron microscopy they showed that the grana repeat distance in spinach thylakoids decreased by 32% (from 212 Å to 144 Å) when the system was illuminated with red light. The observed changes were explained in terms of a change in the internal osmolarity and a change in the membrane thickness following protonation. In [44] it was suggested that the shrinkage of the system induced by illumination occurs in the luminal space because of the increased concentration of  $H^+$ , resulting in a reduction of repulsive forces acting between opposite luminal sides. In [45], a range of complex and interconnected mechanisms are described, including direct protein interactions across the granal lumen, the overall result being a light-induced maximization of the stroma entropy. All these mechanisms focus on grana stack shrinkage, but many of the same mechanisms can occur in the stroma lumen and also, since grana and stroma are intimately connected, a shrinkage in the grana will result in a shrinkage in the stroma lamellar repeat distance, too. We do observe a shrinkage in the stroma repeat distance, up to 23%, depending on light intensity, which is comparable to the effect reported in [43].

In conclusion, our data show that SANS as a non-invasive technique is particularly useful for exploring dynamic changes in-situ in the ultrastructure of thylakoid membranes under different conditions and during their photosynthetic functions. With the availability of high-intensity neutron sources allowing studies on short time-scales SANS can complement electron microscopy techniques and contribute substantially to our knowledge on the structure and flexibility of the multilamellar thylakoid membrane systems.

## Acknowledgements

We wish to thank Thomas Hecksher, Kasper H. Swiatek Renáta Ünnepe and Tünde Tóth for participating in some of the experiments. We also thank Thomas Geue for support during our measurements at PSI. Oda Brandstrup and Ib Høst Pedersen are thanked for logistic and laboratory support. DanScatt (Danish Centre for the use of Synchrotron X-ray and Neutron facilities) is thanked for financial support. The skilful assistance of Piotr Binczycki in preparing the TEM images is gratefully acknowledged. This work was partially supported by the Marie Curie Initial Training Network 'HARVEST' sponsored by the 7th Framework Program of the European Union [No. 238017] and by the Hungarian Scientific Research Fund/National Office for Research and Technology [No. 80345] grants to G.G., National Office for Research and Technology [NAP-VEVEUS05] grant to L.R. and Bourse du Gouvernement Français to G.N.

## References

- [1] L.A. Staehelin, Chloroplast structure: from chlorophyll granules to supra-molecular architecture of thylakoid membranes, *Photosynth. Res.* 76 (2003) 185–196.
- [2] L. Mustárdy, G. Garab, Granum revisited. A three-dimensional model – where things fall into place, *Trends Plant Sci.* 8 (2003) 117–122.
- [3] W. Kuhlbrandt, B. Daum, Electron tomography of plant thylakoid membranes, *J. Exp. Bot.* 62 (2011) 2393–2402.
- [4] E. Shimoni, O. Rav-Hon, I. Ohad, V. Brumfeld, Z. Reich, Three-dimensional organization of higher-plant chloroplast thylakoid membranes revealed by electron tomography, *Plant Cell* 17 (2005) 2580–2586.
- [5] L. Mustárdy, K. Buttler, G. Steinbach, G. Garab, The three-dimensional network of the thylakoid membranes in plants: quasispherical model of the granum–stroma assembly, *Plant Cell* 20 (2008) 2552–2557.
- [6] V. Brumfeld, D. Charuvi, R. Nevo, S. Chuartzman, O. Tsaabari, I. Ohad, E. Shimoni, Z. Reich, A note on three-dimensional models of higher-plant thylakoid networks, *Plant Cell* 20 (2008) 2546–2549.
- [7] G. Garab, C.A. Mannella, Reply: On three-dimensional models of higher-plant thylakoid networks: elements of consensus, controversies, and future experiments, *Plant Cell* 20 (2008) 2549–2551.
- [8] B. Daum, D. Nicastro, J.A. II, J.R. McIntosh, W. Kuhlbrandt, Arrangement of photosystem II and ATP synthase in chloroplast membranes of spinach and pea, *Plant Cell* 22 (2010) 1299–1312.
- [9] J.R. Austin, L.A. Staehelin, Three-dimensional architecture of grana and stroma thylakoids of higher plants as determined by electron tomography, *Plant Physiol.* 155 (2011) 1601–1611.
- [10] B. Andersson, J.M. Anderson, Lateral heterogeneity in the distribution of chlorophyll–protein complexes of the thylakoid membranes of spinach-chloroplasts, *Biochim. Biophys. Acta* 593 (1980) 427–440.
- [11] J.P. Dekker, E.J. Boekema, Supramolecular organization of thylakoid membrane proteins in green plants, *Biochim. Biophys. Acta Bioenerg.* 1706 (2005) 12–39.
- [12] J. Brangeon, L. Mustárdy, The ontogenetic assembly of intra-chloroplastic lamellae viewed in 3-dimension, *Biol. Cell.* 36 (1979) 71–80.
- [13] B.E.S. Gunning, M.W. Steer, *Plant Cell Biology, Structure and Function*, Jones and Bartlett Publishers, London, UK, 1996.
- [14] J.K. Holm, *Structure and Structural Flexibility of Chloroplast Thylakoid Membranes*, IMFUFA, Roskilde University, DK-4000 Roskilde, Denmark, 2004.
- [15] J.J.K. Kirkensgaard, J.K. Holm, J.K. Larsen, D. Posselt, Simulation of small-angle X-ray scattering from thylakoid membranes, *J. Appl. Crystallogr.* 42 (2009) 649–659.
- [16] N. Hodapp, W. Kreutz, Electron density profile determination of bacterial photosynthetic membranes, *Biophys. Struct. Mech.* 7 (1980) 65–95.
- [17] D.I. Svergun, M.H.J. Koch, Small-angle scattering studies of biological macromolecules in solution, *Rep. Prog. Phys.* 66 (2003) 1735–1782.
- [18] G. Pabst, N. Kucerka, M.P. Nieh, M.C. Rheinstadter, J. Katsaras, Applications of neutron and X-ray scattering to the study of biologically relevant model membranes, *Chem. Phys. Lipids* 163 (2010) 460–479.
- [19] J.B. Finean, F.S. Sjostrand, E. Steinmann, Submicroscopic organisation of some layered lipoprotein structures – (nerve myelin, retinal rods, and chloroplasts, *Exp. Cell Res.* 5 (1953) 557–559.
- [20] O. Kratky, W. Menke, A. Sekora, B. Paletta, M. Bischof, Orientierende Röntgen Kleinwinkelmessungen an Chloroplasten von Allium–Porrum, *Z. Naturforsch. B* 14 (1959) 307–311.
- [21] W. Kreutz, Strukturuntersuchungen an Plastiden. 5. Bestimmung der Elektronendichte-Verteilung Langs der Flächennormalen im Thylakoid der Chloroplasten, *Z. Naturforsch. B* 18 (1963) 1098–1104.
- [22] S.J. Singer, G.L. Nicholson, Fluid mosaic model of structure of cell-membranes, *Science* 175 (1972) 720–731.
- [23] D.M. Sadler, X-ray-diffraction from chloroplast membranes oriented in a magnetic field, *FEBS Lett.* 67 (1976) 289–293.
- [24] D.M. Sadler, D.L. Worcester, Neutron-diffraction studies of oriented photosynthetic membranes, *J. Mol. Biol.* 159 (1982) 467–484.
- [25] G. Nagy, D. Posselt, L. Kovács, J.K. Holm, M. Szabó, B. Ughy, L. Rosta, J. Peters, P. Timmins, G. Garab, Reversible membrane-reorganizations during photosynthesis in vivo-revealed by small-angle neutron scattering, *Biochem. J.* 436 (2011) 225–230.
- [26] G. Garab, A. Faludi-Dániel, J.C. Sutherland, G. Hind, Macroorganization of chlorophyll a/b light-harvesting complex in thylakoids and aggregates – information from circular differential scattering, *Biochemistry-US* 27 (1988) 2425–2430.
- [27] D.I. Arnon, Copper enzymes in isolated chloroplasts – polyphenoloxidase in *Beta vulgaris*, *Plant Physiol.* 24 (1949) 1–15.
- [28] N.E. Geacintov, F.v. Nostrand, J.B. Tinkel, J.F. Becker, Magnetic-field induced orientation of photosynthetic systems, *Biochim. Biophys. Acta* 267 (1972) 65–79.
- [29] J.G. Kiss, G.I. Garab, Z.M. Tóth, A. Faludi-Dániel, The light-harvesting chlorophyll a/b protein acts as a torque aligning chloroplasts in a magnetic-field, *Photosynth. Res.* 10 (1986) 217–222.
- [30] C.R. Cantor, P.R. Schimmel, *Biophysical Chemistry, Part II Techniques for the Study of Biological Structure and Function*, W. H. Freeman and Company, 1980.
- [31] G. Nagy, *Structure and Dynamics of Photosynthetic Membranes as Revealed by Neutron Scattering*, Université de Grenoble, Grenoble, 2011.
- [32] J. Barber, An explanation for the relationship between salt-induced thylakoid stacking and the chlorophyll fluorescence changes associated with changes in spillover of energy from photosystem II to photosystem I, *FEBS Lett.* 118 (1980) 1–10.
- [33] R. Standfuss, A.C.T. van Scheltinga, M. Lamborghini, W. Kuhlbrandt, Mechanisms of photoprotection and nonphotochemical quenching in pea light-harvesting complex at 2.5 Å resolution, *EMBO J.* 24 (2005) 919–928.



- [34] P.-A. Siegenthaler, N. Murata, *Lipids in Photosynthesis: Structure, Function and Genetics*, Advances in Photosynthesis, vol. 6, Kluwer Academic Publishers, 1998.
- [35] D.W. Krogmann, A.T. Jagendorf, M. Avron, Uncouplers of spinach chloroplast photosynthetic phosphorylation, *Plant Physiol.* 34 (1959) 272–277.
- [36] D.J. Paolillo, 3-dimensional arrangement of intergranal lamellae in chloroplasts, *J. Cell Sci.* 6 (1970) 243–255.
- [37] J.F. Allen, J. Forsberg, Molecular recognition in thylakoid structure and function, *Trends Plant Sci.* 6 (2001) 317–326.
- [38] J. Barber, Influence of surface-charges on thylakoid structure and function, *Annu. Rev. Plant Phys.* 33 (1982) 261–295.
- [39] W.S. Chow, E.H. Kim, P. Horton, J.M. Anderson, Granal stacking of thylakoid membranes in higher plant chloroplasts: the physicochemical forces at work and the functional consequences that ensue, *Photochem. Photobiol. Sci.* 4 (2005) 1081–1090.
- [40] D. Stock, A.G.W. Leslie, J.E. Walker, Molecular architecture of the rotary motor in ATP synthase, *Science* 286 (1999) 1700–1705.
- [41] S. Izawa, N.E. Good, Effect of salts and electron transport on conformation of isolated chloroplasts. 2. Electron microscopy, *Plant Physiol.* 41 (1966) 544–552.
- [42] G. Nagy, M. Szabó, R. Ünnep, G. Káli, Y. Miloslavina, P.H. Lambrev, O. Zsiros, L. Porcar, P. Timmins, L. Rosta, G. Garab, *Photosynth. Res.* (October 2011), doi:10.1007/s1120-011-9693-6.
- [43] S. Murakami, L. Packer, Protonation and chloroplast membrane structure, *J. Cell Biol.* 47 (1970) 332–351.
- [44] P.A. Albertsson, Interaction between the luminal sides of the thylakoid membrane, *FEBS Lett.* 149 (1982) 186–190.
- [45] J.M. Anderson, W.S. Chow, J. De Las Rivas, Dynamic flexibility in the structure and function of photosystem II in higher plant thylakoid membranes: the grana enigma, *Photosynth. Res.* 98 (2008) 575–587.